Gaussian Beam Propagator Scattering by a Fast Moving Perfectly Conducting Circular Cylinder

Eliran Mizrahi [1], Timor Melamed [2]

Department of Electrical and Computer Engineering, Ben-Gurion University of the Negev, Beer Sheva, ISRAEL

[1] eliranm21@gmail.com

[2] timormel@ee.bgu.ac.il

***Abstract*—This contribution is concerned with deriving the canonical scattering of a time-harmonic electromagnetic Gaussian propagator from a fast moving perfectly conducting circular cylinder under the framework of Einstein's Special Relativity. The incident electromagnetic wave objects in this contribution serve as the basis wave propagators of the frame-based phase-space beam summation method, which is a general framework for analyzing radiation from extended sources. The incident Gaussian beam propagator is readily given by its plane wave spectral representation in the laboratory frame. By utilizing the Lorentz transformation and applying Maxwell's boundary conditions in the co-moving frame, we obtain an exact solution for the scattered fields vector potentials in the form of spectral integrals. The later are evaluated asymptotically for high frequencies (of the incident field) and transformed back to the laboratory frame via the inverse Lorentz transformation.**

I. Introduction

The evaluation of the electromagnetic (EM) scattering comprises the core of many of today's technologies. Many of these applications involve interaction of the incident field with moving objects. Therefore it is significant to obtain faster and more accurate methods of solving EM scattering from moving objects.

The *incident* field transverse components over some planar aperture can be decomposed into a superposition of basis functions that span the field over the aperture. Each of the basis functions can be propagated away from the aperture. The resulting EM wave objects are termed EM *propagators*. By summing up these propagators, the aperture field is represented as a superposition of these propagators. In a scattering scenario the boundary value problem is solved for each propagator and the scattered field is assembled by summing over the resulting scattered fields.

A generic solver for scattering from complex objects requires some approximations, i.e. physical optics or the geometrical theory of diffraction for electrically large scatterers and quasi-static approximations for lower frequencies. Alternatively, by introducing the frame-based phase-space beam summation method, scholars have been able to decompose the aperture field into a set of Gaussian beam propagators (GBP) [1]–[4]. These propagators interaction with large objects depends on the local properties of the scatterer at the incident point, therefore, the interaction of a GBP can be modeled as an interaction with a canonic object having properties similar to the object's local geometry.

II. Problem Definition

The presented contribution concerns with the GBP scattering by a PEC circular cylinder of radius a that uniformly translates in the direction of the x-axis, i.e., having a velocity of $\mathbf{v} = v\mathbf{u}_x$ (see Fig. 1). The incident EM wave is propagating in the positive direction of the x axis and is emanating from an aperture that is located in $x = \bar{x}$, thus, the incident GBP (of $\exp(j\omega t)$) time dependance) is given by the plane wave spectral representation [3] over the spectral variables $\mathbf{k}_t = (k_z, k_y)$

$$\begin{aligned}\mathbf{E}^i(\mathbf{r}, t) &= \frac{1}{(2\pi)^2}\int dk_z dk_y \psi(\mathbf{k}_t)\mathbf{E}_0(\mathbf{k}_t)\times \\ &\qquad \exp\{j\left[\omega t - \mathbf{k}\cdot(\mathbf{r} - \bar{x}\mathbf{u}_x)\right]\},\\ \mathbf{H}^i(\mathbf{r}, t) &= \frac{1}{(2\pi)^2}\int dk_z dk_y \psi(\mathbf{k}_t)\mathbf{H}_0(\mathbf{k}_t))\times \\ &\qquad \exp\{j\left[\omega t - \mathbf{k}\cdot(\mathbf{r} - \bar{x}\mathbf{u}_x)\right]\}, \qquad (1)\end{aligned}$$

where $\mathbf{u}_x$ denotes the unit vector in the x axis direction, $k = \omega/c$ is the free-space wave-number,

$$\begin{aligned}&\mathbf{k} = k_x\mathbf{u}_x + k_y\mathbf{u}_y + k_z\mathbf{u}_z,\ k_x = \sqrt{k^2 - k_y^2 - k_z^2},\\ &\mathbf{E}_0(\mathbf{k}_t) = a_z\mathbf{u}_z + a_y\mathbf{u}_y - (a_z k_z + a_y k_y)k_x^{-1}\mathbf{u}_x,\\ &\mathbf{H}_0(\mathbf{k}_t) = \mathbf{k}\times\mathbf{E}_0(\mathbf{k}_t)/k\eta_0, \qquad (2)\end{aligned}$$

and the (spectral) Gaussian window is given by

$$\begin{aligned}\psi(\mathbf{k}_t) = \frac{-2\pi j}{k\Gamma}\exp\left[j\frac{(k_z - \bar{k_z})^2 + (k_y - \bar{k_y})^2}{2k\Gamma}\right]\times \\ \exp[j(k_z\bar{z} + k_y\bar{y})]. \qquad (3)\end{aligned}$$

In (2), a_z, a_y and $\bar{k}_z, \bar{k}_y$ are the incident GBP parameters which determine the incident field magnitude and beam axis, respectively, Γ which satisfies $\mathrm{Im}\Gamma < 0$ is the synthesis window complex parameter that determines the beam width. Note that the harmonic time dependency is kept in this formulation since we apply in this investigation the space-time Lorentz transformation.

III. Exact Solution

In order to obtain the scattered fields we apply the so called frame hopping technique [5]–[7] in which the incident field is transformed into a co-moving frame (where the scatterer is stationary) via the Lorentz transformation. In the co-moving

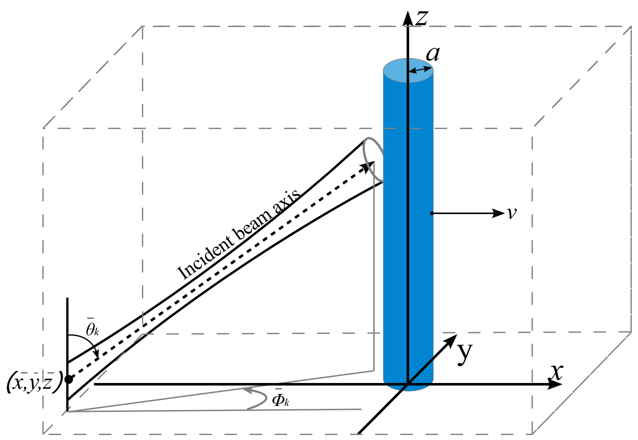

Fig. 1. Physical configuration of the scattering problem. The incident GBP is propagating along the beam axis in the direction of $\bar{\phi}_k = \arctan\left(\bar{k}_y/\bar{k}_x\right)$ and $\bar{\theta}_k = \arccos\left(\bar{k}_z/k\right)$ and impinging on a fast moving PEC cylinder.

frame, the scattered fields are obtained by solving Maxwell's equations with a boundary condition and finally, Lorentz transformation is applied in order to acquire the scattered fields in the laboratory frame.

Under the Lorentz transformation an event (x, y, z, t) in the laboratory frame (the K-frame) is mapped to an event (x', y', z', t') in the co-moving frame (the K'-frame),

$$y' = y, \quad z' = z, \quad t' = \gamma(t - \beta\frac{x}{c}), \quad x' = \gamma(x - vt), \tag{4}$$

where

$$\gamma = (1-\beta^2)^{-\frac{1}{2}}, \ \beta = v/c. \tag{5}$$

and v is the relative velocity between the two frame (the cylinder velocity). The EM fields in K'-frame are transformed in the following manner

$$\begin{aligned} &E'_x = E_x, \ E'_y = \gamma(E_z - \beta\eta_0 H_z), \ E'_z = \gamma(E_z + \beta\eta_0 H_y), \\ &H'_x = H_x, \ H'_y = \gamma(H_y + \frac{\beta}{\eta_0}E_z), \ H'_z = \gamma(H_z - \frac{\beta}{\eta_0}E_y), \end{aligned} \tag{6}$$

therefore, we obtain the incident beam in the co-moving frame

$$\begin{aligned} &\mathbf{E}'^i(\mathbf{r}, t) = \exp\left(j\frac{\omega}{\gamma}t'\right)\exp\left(jk\beta\bar{x}\right)\frac{-j}{2\pi k\Gamma}\int dk_z dk_y \\ &\mathbf{E}'(\mathbf{k}_t)\exp\left[-j(k'_x x' + k_y y' + k_z z')\right]\times \\ &\exp\left\{j\left[\frac{(k_z - \bar{k}_z)^2 + (k_y - \bar{k}_y)^2}{2k\Gamma} + k_z\bar{z} + k_y\bar{y} + k'_x\bar{x}'\right]\right\}, \\ &\mathbf{H}'^i(\mathbf{r}, t) = \exp\left(j\frac{\omega}{\gamma}t'\right)\exp\left(jk\beta\bar{x}\right)\frac{-j}{2\pi k\Gamma}\int dk_z dk_y \\ &\mathbf{H}'(\mathbf{k}_t)\exp\left[-j(k'_x x' + k_y y' + k_z z')\right]\times \\ &\exp\left\{j\left[\frac{(k_z - \bar{k}_z)^2 + (k_y - \bar{k}_y)^2}{2k\Gamma} + k_z\bar{z} + k_y\bar{y} + k'_x\bar{x}'\right]\right\}, \end{aligned} \tag{7}$$

where $k'_x = \gamma(k_x - k\beta)$ and $\bar{x}' = (\bar{x}\gamma^{-1} - vt')$.

In the co-moving frame we approach the EM boundary value problem by first applying a cartesian to cylindric transform for the coordination system,

$$x' = \rho'\cos\phi', \ y' = \rho'\sin\phi', \ z' = z'. \tag{8}$$

Next we apply scalarization to the problem as in [8], we describe the incident EM field in K'-frame with the well known EM vector Hertz potentials which are chosen to be z directed,

$$\mathbf{A}'^i = \Psi'^i_a\mathbf{u}_z, \ \mathbf{F}'^i = \Psi'^i_f\mathbf{u}_z. \tag{9}$$

The relation between the EM fields and the z directed vector potentials in cylindrical coordinates is given by

$$\begin{aligned} E'^i_\rho &= \frac{1}{j\omega'\epsilon_0}\frac{\partial^2\Psi'^i_a}{\partial\rho'\partial z'} - \frac{1}{\rho'}\frac{\partial\Psi'^i_f}{\partial\phi'}, \\ E'^i_\phi &= \frac{1}{j\omega'\epsilon_0\rho'}\frac{\partial^2\Psi'^i_a}{\partial\phi'\partial z'} + \frac{\partial\Psi'^i_f}{\partial\rho'}, \\ E'^i_z &= \frac{1}{j\omega'\epsilon_0}\left(\frac{\partial^2}{\partial^2 z'} + k'^2\right)\Psi'^i_a, \\ H'^i_\phi &= \frac{1}{j\omega'\mu_0\rho'}\frac{\partial^2\Psi'^i_f}{\partial\phi'\partial z'} - \frac{\partial\Psi'^i_a}{\partial\rho'}, \\ H'^i_\rho &= \frac{1}{j\omega'\mu_0}\frac{\partial^2\Psi'^i_f}{\partial\rho'\partial z'} + \frac{1}{\rho'}\frac{\partial\Psi'^i_a}{\partial\phi'}, \\ H'^i_z &= \frac{1}{j\omega'\mu_0}\left(\frac{\partial^2}{\partial^2 z'} + k'^2\right)\Psi'^i_f. \end{aligned} \tag{10}$$

where $\omega' = \gamma(\omega - k_x v)$. From (9) and (10) we note that $\mathbf{A}$ generates a TM field and $\mathbf{F}$ generates a TE field with respect to the z direction.
By comparing (10) with the incident field in (7), we identify the incident vector potential as

$$\Psi'^i_a = \frac{j\omega'\epsilon_0}{k^2_\rho}E'^i_z, \ \Psi'^i_f = \frac{j\omega'\mu_0}{k^2_\rho}H'^i_z. \tag{11}$$

Note that the incident potential is in the form of plane waves spectral integrals, however, in the K'-frame the plane waves temporal frequency varies as a function of the spectral variables $\mathbf{k}_t = (k_z, k_y)$. The boundary value problem for each incident plane wave in the co-moving frame has a well known solution [9] that is obtained by the method of eigenfunction decomposition

$$\begin{aligned} \tilde{\Psi}'^s_a &= -\frac{j\omega'\epsilon_0}{k^2_\rho}\exp(-jk'_z z')\times \\ &\sum_{n=-\infty}^{\infty} j^{-n}\exp\left[jn\left(\phi' - \phi'_k\right)\right]\frac{J(k'_\rho a)}{H^{(2)}(k'_\rho a)}H^{(2)}(k'_\rho\rho'), \\ \tilde{\Psi}'^s_f &= -\frac{j\omega'\mu_0}{k^2_\rho}\exp(-jk'_z z')\times \\ &\sum_{n=-\infty}^{\infty} j^{-n}\exp\left[jn\left(\phi' - \phi'_k\right)\right]\frac{\dot{J}(k'_\rho a)}{\dot{H}^{(2)}(k'_\rho a)}H^{(2)}(k'_\rho\rho'). \end{aligned} \tag{12}$$

where $\phi_k' = \arctan(k_y/k_x')$, J_n and $H_n^{(2)}$ are the n$^{\text{th}}$ order Bessel and the n$^{\text{th}}$ order (second kind) Hankel functions, respectively, and the over dot denotes a derivative with respect to the argument.

By applying the superposition principle to the spectral representation in (11) we obtain the solution for the scattered potentials due to an incident GBP

$$\Psi_a^{'s} = \exp\left(j\frac{\omega}{\gamma}t'\right)\exp(jk\beta\bar{x})\frac{-j}{2\pi k\Gamma}\int dk_z dk_y E_z' \tilde{\Psi}_a^{'s}\times$$
$$\exp\left\{j\left[\frac{(k_z-\bar{k}_z)^2+(k_y-\bar{k}_y)^2}{2k\Gamma}+k_z\bar{z}+k_y\bar{y}+k_x'\bar{x}'\right]\right\},$$
$$\Psi_f^{'s} = \exp\left(j\frac{\omega}{\gamma}t'\right)\exp(jk\beta\bar{x})\frac{-j}{2\pi k\Gamma}\int dk_z dk_y H_z' \tilde{\Psi}_a^{'s}\times$$
$$\exp\left\{j\left[\frac{(k_z-\bar{k}_z)^2+(k_y-\bar{k}_y)^2}{2k\Gamma}+k_z\bar{z}+k_y\bar{y}+k_x'\bar{x}'\right]\right\}. \tag{13}$$

the EM fields are obtained from the potential in three phases, first we apply (10) so to obtain the fields, then we apply a cylindrical to cartesian coordinate transformation, the third phase is to apply the inverse Lorentz transform to obtain the EM fields in K-frame. This is a simple, yet lengthy procedure and therefore, it is not given here.

IV. Asymptotic Solution

In this section we present the asymptotic solution for our problem. Recall that our incident field is given as a Gaussian plane wave spectrum, therefore, our scattered potentials are given as a Gaussian spectrum of scattered potential solutions of the "scattering of a plane wave by a stationary perfectly conducting circular cylinder" problem. These potentials are given in (12). Additionally, for large $k_\rho' a$, by applying Watson transformation on the eigenfunction series and approximating the resulting integral (by applying the steepest descent path and the residue theorem) [10] these potentials are given as a superposition of three types of waves - reflected waves in the light region and an inverse incident waves in the shadow region (which summed up with the incident wave generates a null field in the shadow region) and creeping waves in both the light and shadow regions. These plane wave incidence solutions form the basis of our asymptotic solution.

Note that the Gaussian spectrum of the integrals in (13) is localized about the spectral point $(\bar{k}_z, \bar{k}_y)$. If $\bar{k}_\rho'(\bar{k}_z, \bar{k}_y)$ satisfies $\bar{k}_\rho' a \ll 1$ then we substitute $\tilde{\Psi}_a^{'s}$ and $\tilde{\Psi}_f^{'s}$ in (13) with their asymptotic forms, the integral representation of the solution then becomes a summation of three Fourier integrals one for each wave type. The Fourier integrals are then evaluated asymptotically by the steepest descent path.

The outcome of this procedure is of the following form

$$\Psi_a'(\mathbf{r},t) \sim \exp(j\omega\gamma^{-1}t')\exp(jk\beta\bar{x})\exp(jk\bar{q})$$
$$\frac{k}{(2\pi)}\frac{E_z'\bar{R}}{j\Gamma}\frac{\exp\{jkQ_s\}}{\sqrt{det[\mathbb{H}]}}. \tag{14}$$

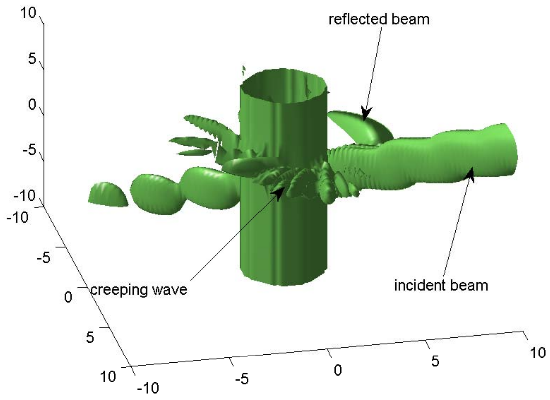

Fig. 2. Equi-magnitude surface of the total magnetic potential for a grazing GBP incidence. the cylinder is of radius $a = 2$ and is stationary The beam parameters are $\Gamma = -10^{-4} - j10^{-1}$, $\bar{k}_z = \bar{k}_y = k/\sqrt{3}$, $\bar{y} = -7$, $\bar{x} = \bar{z} = -10$ and $ka = 200$ such that the incident beam graze the perfectly conducting cylinder. One can identify the incident, the reflected and the creeping waves that arise from such incidence. The creeping wave attenuation constant has been decreased artificially in order for it be observable in this plot, The cylinder surface is plotted as well.

where

$$q = \frac{(\kappa_z-\bar{\kappa_z})^2+(\kappa_y-\bar{\kappa_y})^2}{2\Gamma}+\kappa_y\bar{y}+\kappa_x'\bar{x}'+\kappa_z(\bar{z}-z')-$$
$$\kappa_\rho'\Omega(\mathbf{r}',\bar{\phi}_k'), \tag{15}$$

$$Q_s = -\frac{1}{2}(\nabla\bar{q})^T\mathbb{H}^{-1}(\nabla\bar{q}), \tag{16}$$

$$\mathbb{H} = \begin{pmatrix} \partial_{\kappa_z\kappa_z} & \partial_{\kappa_z\kappa_y} \\ \partial_{\kappa_y\kappa_z} & \partial_{\kappa_y\kappa_y}\end{pmatrix}\bar{q}, \qquad \nabla\bar{q} = \begin{pmatrix}\partial_{\kappa_z} \\ \partial_{\kappa_y}\end{pmatrix}\bar{q}. \tag{17}$$

The upper bar denotes insertion of $\kappa_z = \bar{\kappa}_z$ and $\kappa_y = \bar{\kappa}_y$. The Ω and R function differ between the different types of asymptotic wave (incident, reflected and creeping).

From (14)–(17) we note that the solution magnitude is concentrated about the spatial-temporal regions in which

$$\nabla\bar{q} = 0. \tag{18}$$

Away from these regions the solution magnitude exhibits rapid Gaussian attenuation. The physical interpretation of the solution is derived from equation (18) for the various types of waves.

Through examination of equation (18) interesting high frequency and high speed wave phenomena such as "shifted shadow region", "spiral shaped reflected beam", "creeping bullets", "modulation-frequency Doppler shift" and an "elliptic behavior of the circular scatterer" are observed.

V. Graphical Representation of the Solution

In this section we plot two cases of the total field. The field in Fig. 2 is a 3D representation of the incident, reflected and creeping waves for the stationary cylinder case.

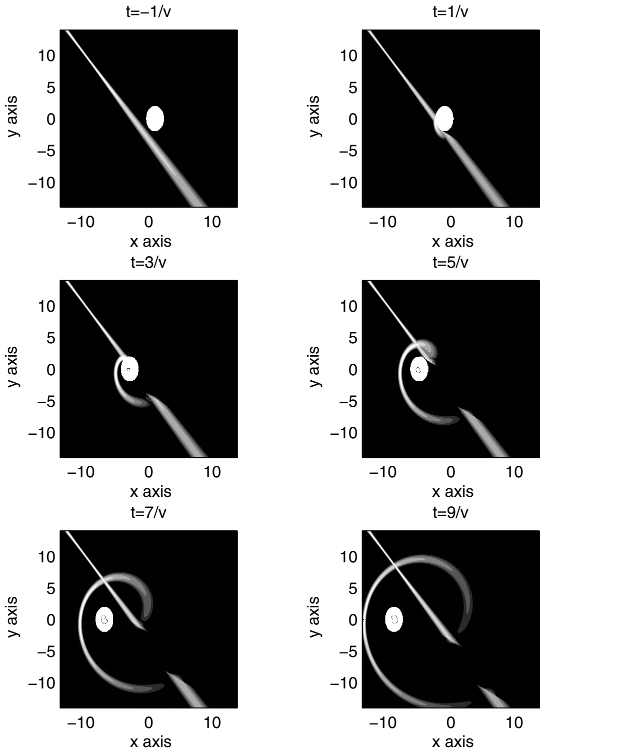

Fig. 3. Total magnetic potentials in K-frame. The cylinder of radius $a = 2$ and is moving in uniform speed of $v = -0.7c$. The beam parameters are $\Gamma = -10^{-4} - j10^{-1}, k = 1000, \bar{k}_z = 0, \bar{k}_y = -0.8k, \bar{y} = 10, \bar{x} = -10$ and $\bar{z} = 0$. These figures clearly demonstrate the incident beam and the spiral shaped reflected beam.

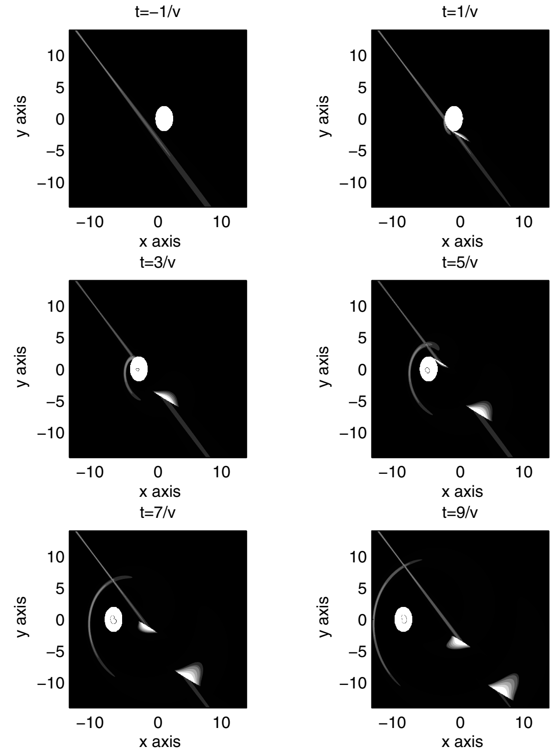

Fig. 4. Total magnetic potentials in K-frame. The problem parameters are as in figure 3. However, in this figure we have artificially multiplied the creeping waves by a factor of 100 and the incident and reflected waves were scaled by a factor of 0.1, in order to make the creeping waves easily notable. Note that the creeping bullets are propagating at the shadow-light boundary and therefore, smooth the transition between light and shadow

In Fig. 3 and 4 the GBP is plotted in K-frame and the cylinder is in a uniform motion. Note that a reflected beam is generated in a propagation direction that dependents on the instantaneous angle between the incident beam and the normal to the cylinder at the incidence point. Due to this time-dependent reflection angle the reflected beam is spiral shaped. In addition, creeping bullets are generated at the moments of grazing incidence and propagate along the shifted light-shadow boundary and smooth solution in this transition region.

VI. Conclusion

In the present contribution the scattering of a GBP by a PEC circular cylinder in uniform motion is solved by using exact spectral representation of the Hertz potentials in the co-moving frame. A numerical illustration of the fields was presented for both the moving and non-moving cylinder cases. This contribution is intended to serve as a building block in the work towards creating a generic relativistic scattering method. The local interactions between the scatterer and the incident propagator as well as the ability to span an arbitrary field using a discrete summation of GBP, points out that the GBP is a very good candidate for such an endeavor.

References

[1] D. Lugara, C. Letrou, A. Shlivinski, E. Heyman, and A. Boag, , "The frame based Gaussian beam summation method: Theory and application," *Radio Science*, vol. 38, 2003.
[2] A. Shlivinski, E. Heyman, A. Boag, and C. Letrou, "A phase-space beam summation formulation for ultra wideband radiation," *IEEE Trans. Antennas Propagat.*, vol. 52, pp. 2042–2056, 2004.
[3] T. Melamed, "Exact beam decomposition of time-harmonic electromagnetic waves," *J. Electromag. Waves Appl.*, vol. 23, pp. 975–986, 2009.
[4] T. Melamed, "Te and tm beam decomposition of time-harmonic electromagnetic waves," *J. Opt. Soc. Am. A*, vol. 28, pp. 401, 2011.
[5] S.W. Lee and R. Mittra, "Scattering of electromagnetic waves by a moving cylinder in free space," *Canadian Journal Of Physics*, vol. 45, 1967.
[6] J. Van Bladel, *Relativity and Engineering*, Springer, N.Y., 1984.
[7] D. Censor, "Application-oriented relativistic electrodynamics (2)," *Progress In Electromagnetics Research*, vol. 29, pp. 107–168, 2000.
[8] R.F. Harrington, *Time-Harmonic Electromagnetic Field*, IEEE Press, John Wiley & Sons, Ins., 605 Third Avenue, NY, 2001.
[9] A. Ishimaru, *Electromagnetic wave propagation, radiation, and scattering*, Prentice-Hall International, London, 1991.
[10] G.L James, *Geometrical Theory Of Diffraction For Electromagnetic Waves*, Inst of Electrical Engineers, London and New York, 1980.